Observation of Internal Damage and Inelastic Deformation of Graphite/Epoxy Tubes $[\pm 45°]_4$ under Cyclic Axial Loading

Y. Kanagawa, T. Ishida, S. Murakami and K. Tanaka

Department of Mechanical Engineering, Nagoya University
Furo-cho, Chikusa-ku, Nagoya 464-01, Japan

ABSTRACT

The effects of stress ratio on the internal damage and the inelastic deformation of graphite/epoxy laminate tubes $[\pm 45°]_4$ under tension-compression cyclic loading are discussed. Cyclic stress-strain curves show viscoelastic-plastic behavior with cyclic hardening and softening, and are largely affected by the evolution of internal damage. Development of matrix cracking and delamination causes the increase of the width of hysteresis loops as a result of the decrease of the elastic modulus and the global stiffness. These phenomena have significant dependence on the stress ratios. In particular, in the case of stress ratio $R(-\sigma_{min}/\sigma_{max}) < 0$, salient and complex inelastic deformations were observed mainly due to the delamination and the resulting local bulging of the tubular specimens. The reduction of Young's modulus is found to reflect the change of the internal damage.

KEY WORDS

composite material, fatigue, inelastic deformation, graphite/epoxy laminate, tubular specimen, stress ratio, cyclic tension-compression, matrix cracking, delamination, internal damage

1. INTRODUCTION

Composite laminates employed in practical engineering components are subject to various non-steady loading under combined states of stress. Thus a number of papers /1-5/ have been published in order to elucidate the mechanisms of damage and fracture of composites under quasi-static or cyclic loading mainly in the range of elasticity.

The laminae of these composites, however, show not only elastic deformation, but also salient inelastic deformation due to stresses in off-fiber directions. The cyclic global loading and the related interlaminar stress induce significant internal damage of matrix cracking, delamination, fiber breakage, and so on.

The present paper is concerned with tension-compression fatigue tests of graphite/epoxy $[\pm 45°]_4$ laminate tubes performed with special emphasis on the evolution of the inelastic deformation observed in the stress-strain hysteresis loops and the related internal damage under a wide range of stress amplitude and stress ratios.

2. MATERIALS AND TEST CONDITIONS

The experiments were performed on the graphite/epoxy

Table 1 Mechanical properties of composite laminate

Young's Modulus	16GPa	Shear Modulus	30GPa
Tensile Yield Stress	130MPa	Compressive Yield Stress	125MPa
Tensile Strength	198MPa	Compressive Strength	170MPa
Shear Strength	420MPa		

laminate tubular specimens shown in Fig. 1. The inside and outside diameters and the gauge length were 15mm, 17mm, and 40mm, respectively. The stacking sequence of the specimens was $[\pm 45°]_4$, fabricated from prepreg Toray P3052 (T300/2500) 0.125mm thick. The volume fraction of the fiber was 59 percent in the prepreg. Table 1 shows the mechanical properties of the specimens employed in this paper.

The tests were carried out under stress-controlled cyclic tension and compression by use of an electrohydraulic servo-controlled tension-compression-torsion machine (Shimadzu EHF-EB-10/TB-20L). The axial strain of the specimen was measured by use of a clip-on type extensometer MTS-632.11-C20 which can measure a maximum measurable strain ± 15%. Strain gauges were not used in order to avoid the influence of heat generation under cyclic loading. The change of specimen diameter was also measured during the tests.

Fatigue tests were performed under constant stress rate of 10 MPa/sec (0.02 - 0.04 Hz) in the ambient atmosphere. Table 2 shows fatigue test conditions of stress ratios $R = \sigma_{min}/\sigma_{max}$ and stress amplitudes σ_a.

Evolution of internal damage was observed at various stages of the fatigue tests. The tubular specimens were cut along the fiber direction of 45° with respect to the specimen axis by use of a diamond circular saw (Maruto MC-100). The surfaces of the sections were then examined by a light surface microscope (Olympas BHM-MU).

3. INELASTIC DEFORMATION OF COMPOSITE LAMINATE TUBES

When the composite laminates are subjected to uniaxial monotonic loading in a direction almost coincident with that of their fibers, they usually show linear elastic behavior. However, in other directions, they may show salient inelastic deformation. Furthermore, when they are subjected to cyclic loading, they show strain hardening of the matrix as well as the softening due to internal damages.

The causes and mechanisms of inelastic deformation will be discussed first in order to elucidate the relationship between the evolution of the internal damage and the concurrent inelastic deformation.

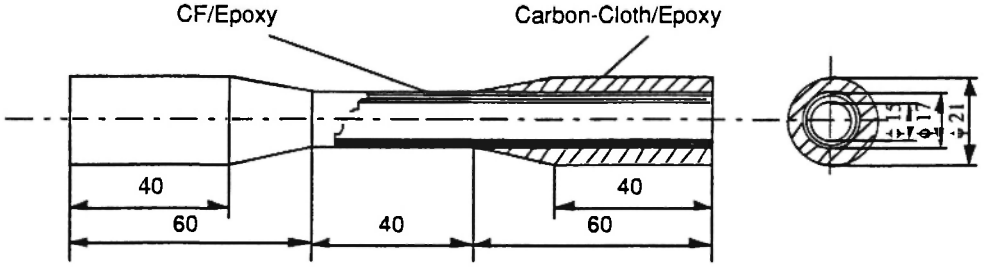

Fig. 1: Composite laminate tubular specimen

Table 2 Stress conditions and number of tests

R \ σ_a	120	105	90	80	75	70	67.5	60
0			3	7	1	3	4	1
-0.25				3	3			
-0.5	1		4	2			1	
-0.75		1			1			
-1	2		2	3			3	
-2			1					
-4				2				
∞				4	1	1	3	2

3.1. Mechanisms of Inelastic Deformation

Fatigue tests were performed on the tubular specimens of Fig. 1 under five different stress ratios R (= $\sigma_{min}/\sigma_{max}$) = 0, -0.25, -1, -4 and ∞ for a constant stress amplitude σ_a = 80 MPa. The resulting hysteresis loops of the stress strain curves are shown in Fig. 2.

As observed in these figures, hysteresis loops show significant non-linearity, and the shape of the loops changes largely in the process of fatigue. It is known that graphite fibers show linear elastic behavior under tension up to fracture, but the elastic limits for the compressive stress in the fiber direction and for the shear stress parallel to the fibers are far smaller than that for tension. Thus the causes of the non-linear behavior in Fig. 2 may be attributable to the following five factors:

1. Viscoelastic-plastic deformation of the epoxy resin for the matrix and the interlaminar adhesive.
2. Development of microscopic cracking in the epoxy resin for the matrix and the interlaminar adhesive.
3. Delamination induced by crack growth in the lamina interface.
4. Debonding at the fiber-matrix interface and fiber breakage.
5. Reduction of bending rigidity induced by the development of delamination, and the resulting local bulging and global buckling due to compressive loading.

Factors 1 and 2 are related to the mechanical properties of the epoxy resin, and resulting strain-hardening during the cyclic viscoelastic-plastic deformation as well as in strain softening due to the initiation of microcracking. Factors 3, 4 and 5, on the other hand, are concerned with the structure of composite materials. Factor 3 is induced mainly by the shear stress between laminae, while 5 is related not only to the mechanical properties of the composite laminate, but also to the geometry of the laminate tube.

The salient and significant changes of hysteresis loop in the fatigue process of the tubular specimen shown in Fig. 2 can be interpreted in terms of these five factors.

3.2. Plastic Property of the Material

In order to discuss the effects of the above factor 1, the inelastic strain in the off-axis composite materials should be separated into the viscoelastic and plastic strains. For this purpose, we first examine the plastic property of the material by performing quasi-static

tension and compression tests. The stress rate in the tests was 10 MPa/sec, identically with the succeeding fatigue tests. Thus the effects of rate dependence were disregarded in this paper.

Specimens were loaded monotonically to a specified stress, and then unloaded to zero. The plastic strain was determined from the residual strain at 24 hours after the unloading, since viscoelastic strain essentially recovers in this period. The yield stress of the materials was specified by the proof stress of 0.2% plastic strain. The resulting yield stresses for tension and compression were σ_{yt} = 130 MPa and σ_{yc} = 125 MPa, respectively, as entered in Table 1.

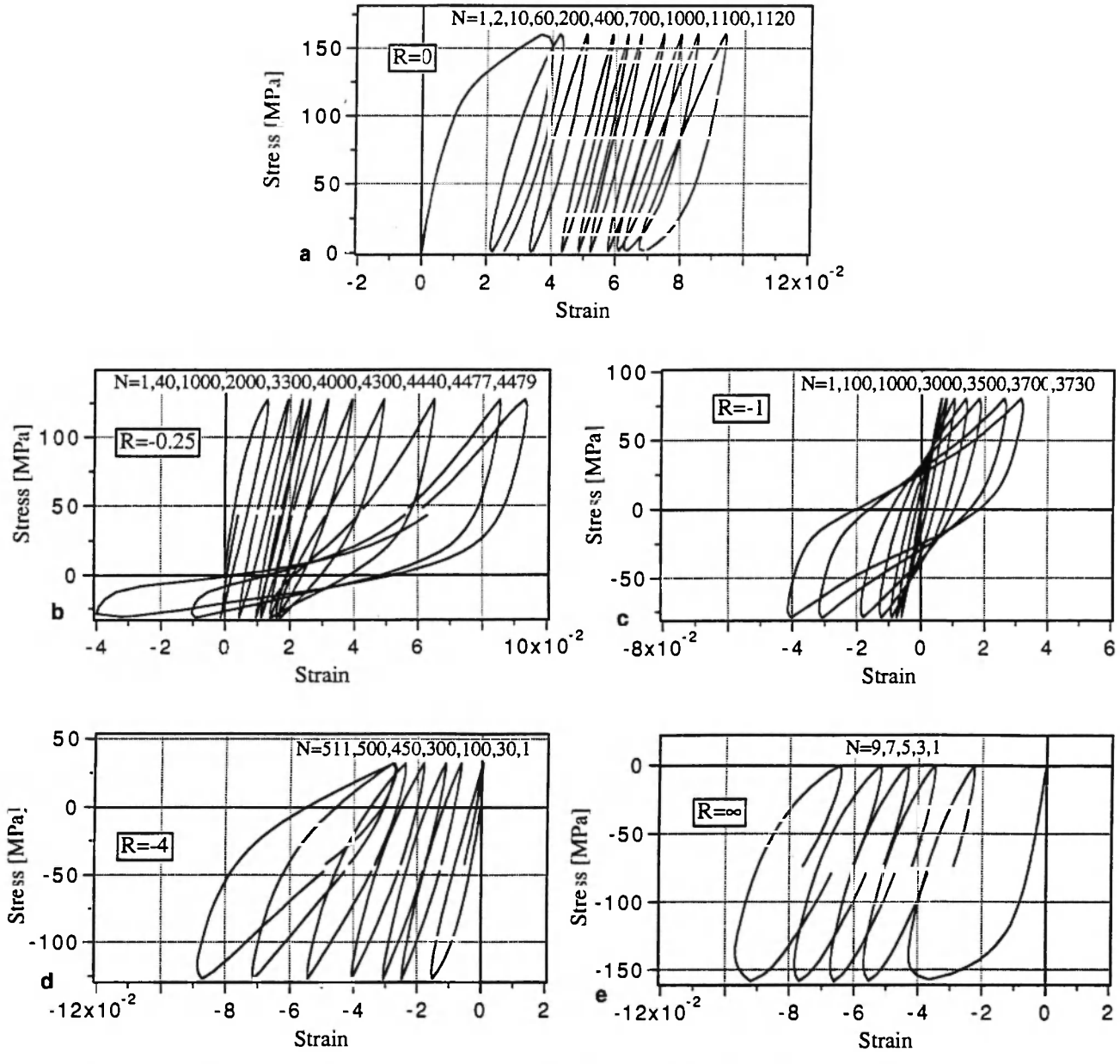

Fig. 2: Cyclic stress-strain loops under various stress ratios with constant stress amplitude σ_a = 80 MPa.

4. CHANGES OF INELASTIC DEFORMATION AND YOUNG'S MODULUS OF COMPOSITE LAMINATE TUBES IN FATIGUE PROCESS

The changes of elastic and inelastic properties will be discussed in relation to the internal damage induced in the process of fatigue. The effects of stress ratios on damage and deformation will be elucidated.

4.1. Cyclic Inelastic Deformation for Stress Ratio R = 0

Fig. 2(a) shows the cyclic stress-strain hysteresis loops for the stress ratio R = 0 and the average stress σ_a = 80 MPa. In this case, the maximum stress is σ = 160 MPa which is larger than the yield stress of 130 MPa shown in Table 1. Therefore the stress-strain relation in the first cycle N = 1 shows a large inelastic behavior due to viscoelastic and plastic deformation of the matrix of each lamina and interlaminar adhesive.

The maximum strain is observed during the unloading stage after the maximum stress. That is, the stress-strain relation in the unloading process shows salient non-linear behavior, and the residual strain of about 2% is observed in the first cycle, as a result of plastic and viscoelastic deformation of the material.

As the yield stress increases due to the plastic strain in the N = 1 cycle, plastic deformation does not occur in the N = 2 cycle, and thus the inelastic strain in the cycle N = 2 consists mainly of viscoelastic strain. Because of the strain hardening of the resin due to stress cycles, the cycles N ≥ 3 show smaller hysteresis loops in addition to significant cyclic creep strain due to the positive average stress.

The rate of cyclic creep and the width of the loop decrease up to N = 200, i.e. 18% of the fatigue life, N_f = 1123. The width of the loop increases gradually until N = 1000 (i.e., N/N_f = 0.89), and then it starts to increase again. The change in this stage is induced mainly by the delamination, as will be discussed in Fig. 5 in Section 5. The initiation and the growth of this delamination lead to salient matrix cracking and fiber-matrix debonding, and bring about a decrease in Young's modulus.

In this final stage, the stiffness of the material at stresses of nearly 0 in the unloading process decreases significantly, and thus the slope of the stress-strain loops also decreases. Because of the internal stress in the laminates, local compressive stress may occur at the global stresses of small positive magnitude. This local compressive stress, combined with the decrease of the bending stiffness of the delaminated tubular specimen, will give rise to local bulging and macroscopic buckling of the tube, and this may explain the above significant decrease in the slope of the stress-strain hysteresis curve. The initiation of local bulging was confirmed by increase of the specimen diameter. The development of the internal damages in this test will be discussed in Section 5.

4.2. Cyclic Inelastic Deformation for Stress Ratio R = -0.25

Fig. 2 (b) shows the cyclic stress-strain hysteresis loops for the stress ratio R = -0.25 and stress amplitude σ_a = 80 MPa. Because the maximum stress σ = 128 MPa in the cycle N = 1 is smaller than the tensile yield stress σ_{yt} = 130 MPa, the hysteresis behavior is mainly due to the viscoelastic deformation. Similarly, as in the case of R = 0, cyclic hardening (decrease in the width of hysteresis loop) is observed in the first stage, and the concurrent cyclic creep develops as a result of positive average stress. After N = 1000 (N/N_f = 0.22), the width of the loop increases gradually until the N = 3300 cycle (N/N_f = 0.74). This is attributable to the softening of the materials due to matrix cracking (Figs. 3 and 4).

After the N = 3300 cycle, in addition to the reduction of Young's modulus in tensile loading, salient reduction of stiffness is observed in the unloading and the reversed loading process due to the development of matrix cracking and delamination; this leads to a rapid increase of the width of the loop. The increase of the width of the hysteresis loop is far more significant for the reverse loading (σ < 0) of the case of R = -0.25 than in the case of R = 0 of Fig. 2 (a).

As regards the stress-strain hysteresis after the N = 4000 cycle (N/N_f = 0.89), the first part of the unloading branch, i.e., the unloading process after the maximum stress to the stress around the average stress shows almost similar behavior to that of the early stages of the

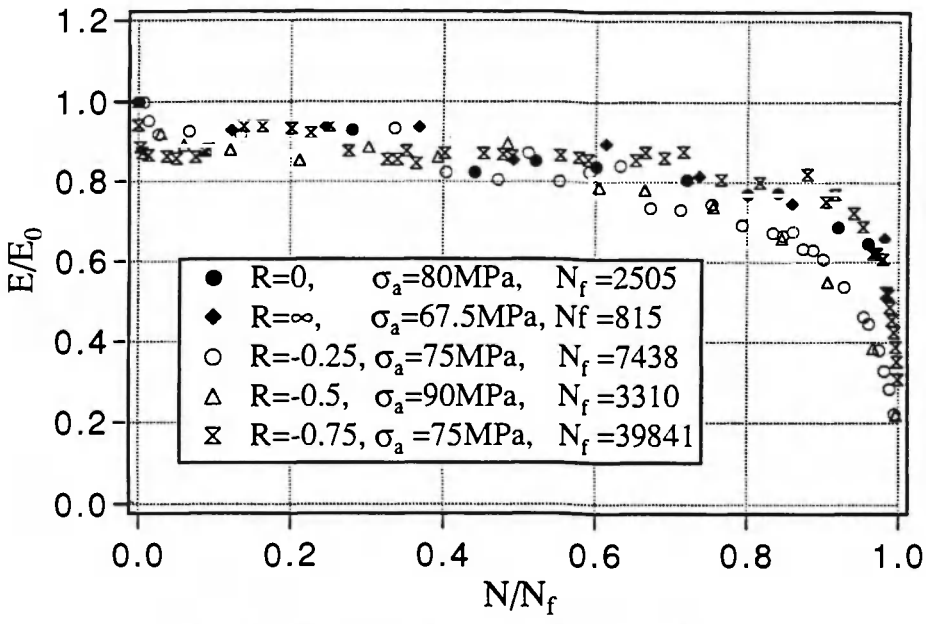

Fig. 3: Young's modulus reduction due to fatigue

(a) N/N_f =0.50

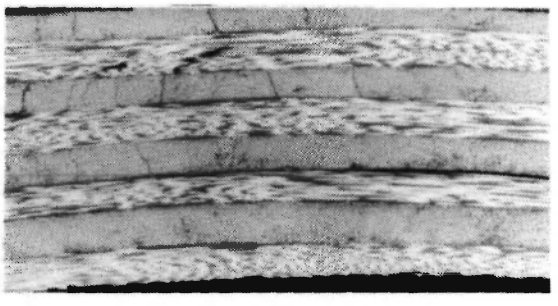

(b) N/N_f =0.80

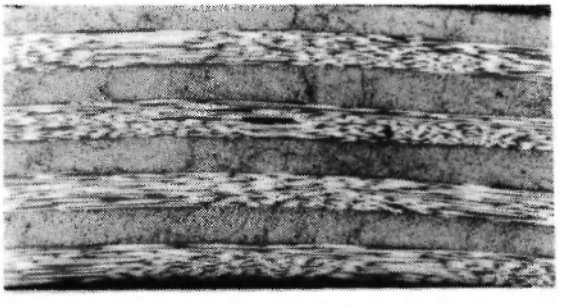

(c) N/N_f =0.96

Fig. 4: The stage of the evolution of internal damage due to fatigue under stress ratio R = -0.25, stress amplitude σ_a = 80 MPa

cyclic test. However, the branches of unloading below the mean stress and those of the reversed loading show a significant decrease of the stiffness, and a significant strain change is observed. This may be attributable to the above mentioned local bulging of the tube specimen whose bending stiffness has been decreased because of the development of the delamination between lamina tubes, as will be observed in fig. 4 (c). Thus, the deformation of the specimen in this stage under axial load consists of the axial bending strain caused by the bulging in addition to that due to axial membrane deformation. In the reloading branch after minimum stress, deformation with low stiffness is again observed. That is, the branches of significantly low stiffness in the hysteresis loops of the stress range around 0 are related mainly to the local bulging of the laminate tube softened by delamination.

4.3. Cyclic Inelastic Deformation for Stress Ratio R = -1

Fig. 2(c) shows the cyclic stress-strain hysteresis loops for the stress ratio R = -1. Since the maximum stress σ_{max} = 80 MPa in this case is half of that of the case of R = 0 and much smaller than the yield stresses σ_{yt} and σ_{yc}, the cyclic loading is in the range of elasticity; plastic and viscoelastic strains are hardly observed in the first cycle N = 1. Thus the slight increase of the loop width in the later stage is attributable to the development of internal damages, i.e., matrix cracking and delamination.

For cyclic loading after N = 3500 (N/N_f = 0.94), a significant decrease of stiffness is observed in the unloading and reverse loading branches at stresses around 0. This may again be explained by the local bulging of the above mentioned tube.

4.4. Cyclic Inelastic Deformation for Stress Ratio R = -4

Fig. 2(d) shows the hysteresis loops for the stress ratio R = -4. Since the mean stress is compressive, cyclic creep develops in the compressive direction. Deformation behavior is similar to that in the case of R = -0.25. However, in the case of R = -0.25, the numbers of the cycle of starting increase of loop width, that of the start of decreasing compressive stiffness due to delamination and that of the fatigue life are N = 1000, 3200 and 4480, respectively, while the corresponding cycle numbers for the case of R = -4 reduce to N = 30, 300 and 512, respectively. That is, damage development under compressive stress is much faster than under tensile stress, the reason being discussed in Section 5.

4.5. Cyclic Inelastic Deformation for Stress Ratio R = ∞

As observed in Fig. 2 (4), the cyclic loading in the case of R = ∞ shows behavior similar to that for R = 0. Since the maximum compressive stress in this case (σ = 160 MPa) is larger than the compressive yield stress σ_{yc} = 125 MPa, the first cycle shows significant plastic and viscoelastic deformation. The hysteresis loops after N = 2 show salient cyclic creep due to the compressive mean stress, in addition to the significant viscoelastic cyclic strain.

The maximum compressive stress 160 MPa in this case is about 95% of the fracture strength in compression of 170 MPa, and thus matrix cracking and fiber fracture occur rapidly under the cyclic loading (Fig. 5). The characteristic marked reduction of stiffness due to the delamination observed in Fig. 2 (b)-(d) did not appear in this case, because the local bulging of the tubular specimen due to delamination led catastrophically to final fracture due to global buckling. For the lower stress level, however, the increase of the loop width and the stiffness reduction were also observed in this case.

4.6. Reduction of Young's Modulus

Fig. 3 shows the reduction of Young's modulus in the course of the fatigue tests under different loading conditions. Young's modulus was measured periodically in the fatigue test by performing local unloading in the stress range of 0-20 MPa to avoid plastic and viscoelastic effects. In order to compare the change of Young's modulus for different stress

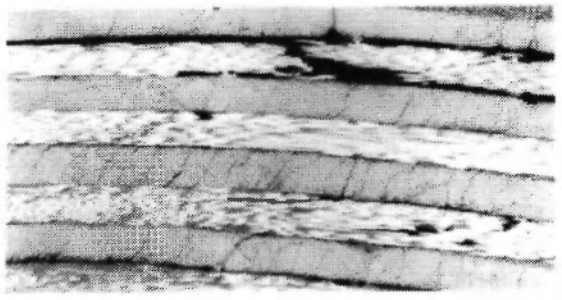

(a) σ_a = 80 MPa, R = 0, N/N$_f$ =0.96

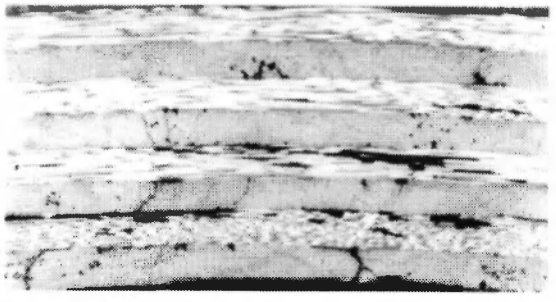

(b) σ_a = 80 MPa, R = ∞, N/N$_f$ =0.94

Fig. 5: Internal damage under stress ratio R = 0 and ∞

conditions, the normalized relation between the non-dimensional modulus E/E_0 and the fatigue life N/N_f were used in Fig. 3, where E_0 is the incipient elastic modulus measured before the test.

As observed in Fig. 3, E/E_0 in the case of R = 0 and R = ∞ decreased gradually up to the stage of N/N_f = 0.9. When E/E_0 had decreased to 60% of its initial value, its rapid drop led to fracture of the specimen. In the cases of R < 0, i.e., R = -0.25, -0.5 and -0.75, on the other hand, E/E_0 decreased gradually up to 0.8. Then, after the fast development of internal damages due to delamination, the specimens broke when E/E_0 had decreased to 20% of its initial value.

Despite some scattering of the results, Fig. 3 shows that the normalized relations between $E/.E_0$ and N/N_f for different R have an almost identical evolution. Moreover, since the values of E/E_0 can be measured accurately at every stage, we can use them as a convenient measure to estimate the damage state and the residual life of each stage.

5. OBSERVATION OF INTERNAL DAMAGE

To elucidate in more detail the relation between the change of hysteresis behavior, the reduction of elastic moduli and the above mentioned internal damage, we further performed microscopic observations on sections of the tubular specimens. The damage process for the three typical stress ratios of R = -0.25, 0 and ∞ will be discussed. To avoid the effects of data scattering, the damage state (life ratio N/N_f) during the fatigue test was estimated from the attained results not only of elastic modulus, but also of the maximum and the minimum strains in the hysteresis loops.

5.1. Evolution of Internal Damage under Cyclic Tension-Compression (R = -0.25)

Fig. 4 shows micrographs of the internal damage for the loading condition of σ_a = 80 MPa and R = -0.25, corresponding to the damage process of Fig. 2 (b).

Fig. 4 (a), to begin with, is the micrograph of the first stage of the damage at the life ratio N/N_f = 0.5, which corresponds to N = 2000 in Fig. 2 (b). Matrix cracking and small fiber breakage can be observed in this figure, but the damage in this stage is still local and diverse. Fiber breakage is observed mainly in the inner layers of the laminate. This stage corresponds to the steady and stable hysteresis loop which corresponds to the minimum width of hysteresis loop. Thereafter, matrix cracking and fiber breakage are gradually accelerated. The change of the shape of the loops and the change of stiffness are still small.

Fig. 4 (b), on the other hand, shows the internal damage of the stage of N/N_f = 0.80 [N = 3300 in Fig. 2 (b)]. There is not only an increase of the densities of matrix cracking and fiber breakage, but they have already developed over the whole cross section of the specimen. Delaminations are found in the heavily damaged area. In this stage, bonding between the laminae has been weakened due to the start of delamination, and the total stiffness of the laminate

tube has decreased and leads to local bulging under compressive load.

The damaged state of $N/N_f = 0.96$ [corresponding to N = 4300 in Fig. 2 (b)] is shown in Fig. 4 (c), where heavy matrix cracking and delamination are observed all over the section. Breaking of the layers themselves is also found in some places. Because of the loss of bonding between layers and the occurrence of delamination, relative rotation and sliding between layers induces significant degradation in the stiffness of the material. In this stage, when the global stress approaches 0 in the process of unloading, each layer deforms as the bulging of a thin cylinder under axial stress, and induces a large reduction of the stiffness of the tube.

5.2. Evolution of Internal Damage Under Cyclic Tension (R = 0)

Micrographical observations in the cases of R = 0 and R = ∞ for σ_a = 80 MPa were also performed to examine the effects of stress ratio on the evolution of internal damage.

Fig. 5 (a) is the internal damage caused in the test of R = 0 at $N/N_f = 0.96$ [N = 1100 in Fig. 2 (a)]. In contrast to the cases of R = -0.25 [Fig. 4 (c)] and R = ∞ [Fig. 5 (b)] below, the development of internal damage is much stronger in this case. As described already, final fracture in the case of R < 0 is brought about by the macroscopic buckling under compressive loading due to the significant reduction of stiffness induced by the delamination. However, final fracture in the case of R = 0 is mainly caused by fiber rupture under maximum tensile stress. Because of the difference in the mechanisms of deformation, the effects of matrix cracking and delamination on the final fracture in the case of R = 0 are smaller than in the cases of R < 0, and, therefore, the specimen does not break until a state of heavy damage is attained. This explains why the more highly damaged state of Fig. 5 (a) is observed in this case than in that of Fig. 4 (c), Fig. 5 (b) under the same stress amplitude but of different stress ratios R.

5.3. Evolution of Internal Damage under Cyclic Compression (R = ∞)

Finally, Fig. 5 (b) shows the internal damage of a specimen of the same life ratio $N/N_f = 0.94$ as in Fig. 5 (a), but under cyclic compression R = ∞ and $|\sigma_{max}|$ = 160 MPa. Damage in this case is predominantly by fiber breakage occurring along the boundary between four inner laminae. Though matrix cracking and delamination are also observed in this case, the number of these defects is small. Because of the high cyclic compressive stress, fiber breakage results from local bulging of the fibers. Then this fiber breakage leads to delamination because it occurs near the laminae interface, and sudden macroscopic buckling occurs in the tubular specimen leading to final fracture. When the compressive stress is small, however, the number of fibers broken decreases but matrix cracking occurs more significantly, and the remarkable inelastic deformation will be observed due to the occurrence of delamination, as in the case of the cyclic tension tests (R = 0).

6. EFFECTS OF STRESS AMPLITUDE AND STRESS RATIO ON FATIGUE LIFE

As already observed in the preceding sections, the difference in damage states under different loading conditions suggests that the development of individual damage is largely dependent on the stress ratio and the stress amplitude. Therefore, Fig. 6 shows the relation between the maximum stress and the number of life cycles with stress ratio as a parameter. It will be observed from this figure that the fatigue lives are largely governed by the maximum stress in laminated composites, rather than by the stress amplitude. This feature may be different from that observed in metals for which the stress amplitude or strain amplitude is the governing factor of fatigue life. The deleterious effects on fatigue lives is more significant in the cyclic loading tests with stress reversal R < 0 than in the cases of cyclic compression (R < ∞). That is, the local bulging

of thin tubular specimens of R < 0 causes salient inelastic deformation and accelerates the evolution of delaminations, and then it may result in shortening of the fatigue life. Therefore, the fatigue lives under various loading conditions may be reasonably classified into three characteristic damage mechanisms shown schematically by the three hatched areas in Fig. 6.

Region A, hatched by vertical lines, representing the loading condition of cyclic tension-compression with high stress level, shows sudden fracture of specimens due to the local disperse defects without significant progressive damage. In region B of cyclic tension-compression at rather low stress levels, hatched by horizontal lines, the final fracture results from the degradation of the composite materials due to accumulation of progressive damage.

In region C for the stress reversal R < 0, hatched by small dots, on the other hand, final fracture is caused by the macroscopic buckling of a thin tubular specimen resulting from the remarkable delamination over the whole range of stress level. The stress-fatigue life relation of stress ratio R = -0.25 (marked by Δ in Fig. 6) almost coincides with that of R = ∞. Though the loading condition of R = -0.25 includes a small amount of compressive stress state, the fatigue life decreases because of the salient inelastic deformation due to local bulging of tubular specimens.

7. CONCLUSIONS

Cyclic tension-compression tests were performed on graphite/epoxy $[\pm 45°]_4$ laminate tubes. The relation between the change of the elastic and inelastic properties and the development of the internal damage was discussed in relation to the loading conditions. The results elucidated in this paper may be summarized as follows:

1. The cyclic stress-strain relations show salient hysteresis loops as a result of the viscoelastic-plastic laminate behavior together with cyclic hardening and damage softening of the matrix. The evolution of internal damage depends significantly on the cyclic loading conditions; the development of delamination is faster in the cyclic tension-compression tests (stress ratio R < 0) than in the cyclic tension tests (stress ratio R > 0).
2. In the cases of cyclic tension-compression tests R < 0, the compressive stiffness of specimens decreases

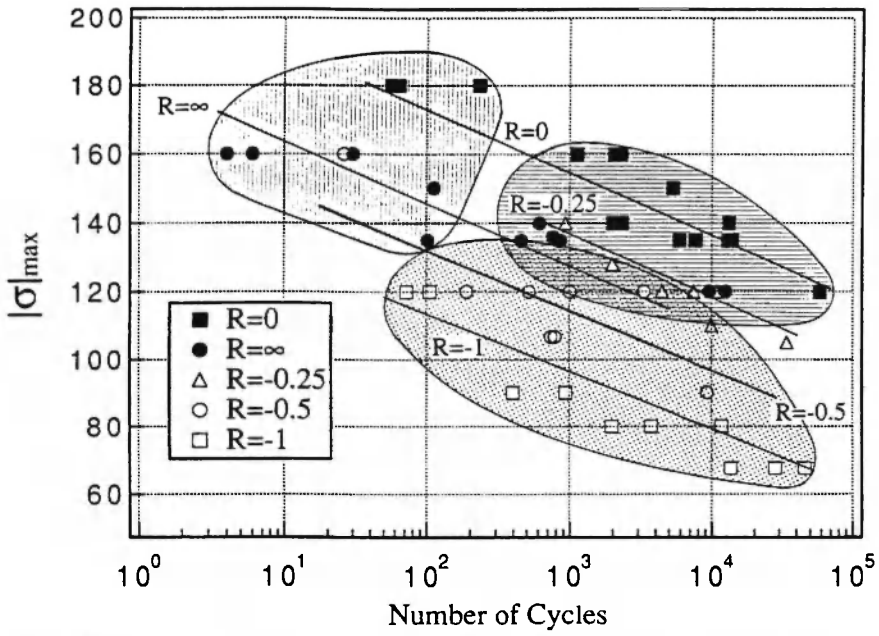

Fig. 6: Fatigue limit under axial cyclic loading and the effect of maximum (or minimum) stress

largely due to the occurrence of delamination, and thus the macroscopic buckling and large inelastic deformation occur.

3. The fatigue of the present composite is governed by the maximum stresses, rather than the stress amplitude. Furthermore, the damage development in cyclic loadings is strongly affected by the stress ratio. Thus the fatigue lives under various loading conditions may be reasonably classified into three characteristic damage mechanisms by the values of the maximum stresses and the stress ratios.

ACKNOWLEDGEMENT

A part of this work was supported financially by a Grant-in-Aid for Scientific Research B [No. 0452099] for the fiscal years from 1990 to 1992 and Grant-in-Aid for Development Scientific Research B-1 (No. 04555029) for 1992 and 1993. The authors would like to express their appreciation for this support.

REFERENCES

1. K.L. Reifsnider, K. Schulte and J.C. Duke, ASTM STP 813, 136 (1984).
2. I.M. Daniel and A. Charewicz, *Engineering Fracture Mechanics*, **25** (6), 793 (1986).
3. T.K. O'Brien, *J. American Helicopter Society*, **32** (13), 13 (1987).
4. A. Rotem, *J. Composites Technology & Research*, **11** (2), 59 (1989).
5. G.Z. Voyiadjis, Damage in Composite Materials, Elsevier Science Publishers B.V., 1993.
6. S. Amijimaa, T. Fujii and T. Sagami, *ASME J. Energy Resources Technology*, **113**, 235 (1991).
7. E. Krempl and T.M. Niu, *J. Composite Materials*, **16**, 172 (1982).
8. K.L. Reifsnider, Handbook of Composites (ed. C.T. Herakovich and Y.M. Tarnopol'skii), 2, Elsevier Science Publishers B.V., 1989, p. 231.
9. H. Tobushi, S. Narumi and K. Osawa, *Bull. JSME*, **29** (248), 348 (1986).
10. H. Tobushi, Y. Ohashi and K. Osawa, *Bull. JSME*, **29** (257) , 3665 (1986).